Characterization of gamma–ray tracking arrays: a comparison of GRETINA and Gammasphere using a ^{60}Co source

T. Lauritsen[a], A. Korichi[b], S. Zhu[a], A.N. Wilson[c], D. Weisshaar[d], J. Dudouet[e], A.D. Ayangeakaa[a], M.P. Carpenter[a], C.M. Campbell[f], E. Clement[h], H.L. Crawford[f], M. Cromaz[f], P. Fallon[f], J.P. Greene[a], R.V.F. Janssens[a], T.L. Khoo[a], N. Lalović[k,i], I.Y. Lee[f], A.O Macchiavelli[f], R.M. Perez-Vidal[g], S. Pietri[i], D.C. Radford[j], D. Ralet[b], L. Riley[l], D. Seweryniak[a], O. Stezowski[e]

[a]*Argonne National Laboratory, Argonne, Illinois 60439, USA*
[b]*C.S.N.S.M, IN2P3-CNRS, bat 104-108, F-91405 Orsay Campus, France*
[c]*University of the West of Scotland, Paisley, UK*
[d]*NSCL, Michigan state University, USA*
[e]*I.P.N. Lyon, IN2P3-CNRS, Lyon Campus, France*
[f]*Lawrence Berkeley National Laboratory, Berkeley, CA 94720, USA*
[g]*Instituto de Fisica Corpuscular, CSIC-Universitat de Valencia, E-46920 Valencia, Spain*
[h]*GANIL, CEA/DSM-CNRS/IN2P3, BP 55027, F-14076 Caen, France*
[i]*GSI Helmholtzzentrum für Schwerionenforschung GmbH, D-64291 Darmstadt, Germany*
[j]*Physics Division, Oak Ridge National Laboratory, Oak Ridge, Tennessee 37831, USA*
[k]*Department of Physics, Lund University, SE-22100 Lund, Sweden*
[l]*Ursinus College, Collegeville, PA 19426, USA*

Abstract

In this paper, we provide a formalism for the characterization of the tracking arrays with emphasis on the proper corrections required to extract their photopeak efficiencies and peak–to–total ratios. The methods are first applied to Gammasphere, a well characterized 4π array based on the principle of Compton suppression, and subsequently to GRETINA. The tracking efficiencies are then discussed and some guidelines as to what clustering angle to use in the tracking algorithm are presented. It was possible, using GEANT4 simulations, to scale the measured efficiencies up to the expected values for the full 4π implementation of GRETA.

Keywords: Segmented germanium detectors, efficiency measurements, γ–ray tracking, Gammasphere, GRETINA, GRETA, γ–ray spectroscopy, nuclear structure.

Contents

Email address: torben@anl.gov (T. Lauritsen)

Appendix B Range of γ rays in Ge 12

1. Introduction

The concept of escape suppression revolutionized the field of γ-ray spectroscopy, enabling significant increases in the resolving power of germanium-based detector arrays [1–3]. Now, the new concept of γ-ray tracking and recent advances in germanium (Ge) crystal segmentation technology are leading to another revolution where escape suppression shields are removed and only Ge crystals are used, filling as much of the space around the source of γ rays as possible [4].

The tracking concept is based on the ability to locate, within a few mm, each photon interaction point in the Ge detector and, consequently, to track the scattering sequence of an incident photon through the crystals. The method consists in the reconstruction of the full γ-ray energy by combining the appropriate interaction points [5–9].

This approach provides a significant gain in detection efficiency over escape-suppressed arrays because the Compton suppression shields (which limit the Ge solid angle) are removed and replaced by active Ge detectors. For the first time, a nearly 4π sphere of Ge, with a good peak–to–total ratio, becomes possible. Moreover, the tracking technique provides identification of the first interaction point with good angular resolution and, therefore, allows for an improved Doppler correction. The expected performance for tracking detector arrays are thus well beyond those of escape-suppressed spectrometers like EUROBALL [10] and Gammasphere [11, 12]. The most advanced implementations of this concept to date are the two arrays AGATA (Advanced GAmma Tracking Array) [13] and GRETINA (Gamma Ray Energy Tracking In beam Nuclear Array) [14]. GRETINA is the early implementation of GRETA (Gamma Ray Energy Tracking Array) [15]. These arrays are built from large, segmented crystals of hyper-pure germanium (HPGe) and are the first to use the concept of γ-ray energy tracking. This technique enables experiments probing low cross sections and/or measurements using high–velocity reaction products like those possible with stable and radioactive beams at new facilities such as SPIRAL2 [16], SPES [17], GANIL [18] and FAIR[19] in Europe and ATLAS/CARIBU [20], NSCL [21] and FRIB [22] in the USA.

The resolving power of a γ-ray detector array (*i.e.*, its ability to isolate a given sequence of γ rays in a complex spectrum) depends on four main properties [23]: efficiency, energy resolution, peak–to–total ratio (P/T) (the ratio of photopeak efficiency to the total efficiency [24]), and granularity. The GRETINA array, and the future 4π array GRETA, are being designed to maximize each of these properties. As these new systems begin to be used in experimental campaigns, it is important that their performances be evaluated accurately. While Monte Carlo simulations using GEANT4 can be used to some extent for this purpose, simulations require precise knowledge of all the detector parameters, such as geometry, mounting hardware and materials other than germanium. Furthermore, results of simulations require validation through measurements.

However, measurements – particularly those related to efficiency calibrations – represent a challenge for tracking arrays, and need to be fully understood and carried out carefully. Both the efficiency and (P/T) depend on parameters that determine whether a tracking algorithm associates a set of interaction points with a single γ ray, multiple γ rays, or a scattered γ ray with partial energy collection. Thus, no single, absolute value of either quantity can be measured. Instead, one must examine the correlation between efficiency and (P/T) in order to find conditions that optimize both.

This paper describes possible ways to determine array efficiencies, with an emphasis on the proper corrections, and explores how different methods compare. We use a ^{60}Co source to obtain efficiencies at 1333 keV; because this is a multiplicity two source (*i.e.*, it emits two γ rays), we also investigate the required correction terms. First, we describe in detail the different methods proposed. Each approach is then validated using data from a well–understood, Compton–suppressed 4π array: Gammasphere. The approaches are then applied to data obtained with GRETINA in two geometries, one at Argonne National Laboratory (ANL) and one at Michigan State University (MSU). At the time of the measurements, the Gammasphere array consisted of 95 escape-suppressed Ge detectors; the results reported below have, therefore, been scaled to provide the characteristics of the more standard 100 detector set-up. GRETINA was comprised of seven quad modules (28 crystals) in compact setups at its nominal distance (18.5 cm from the center position of the array to the front of the Ge crystals) [14]. The results for the tracking array is then scaled to the future full 4π implementation (GRETA) in order to compare the performance with Gammasphere.

2. Efficiency and peak–to–total ratio measurements

The photopeak efficiency, ϵ_p, is defined as the probability that a single emitted γ ray is measured in the photopeak in the spectrum. The total efficiency, ϵ_T, is defined as the probability that a γ ray adds one or more counts anywhere in the spectrum. The ratio of these efficiencies is known as the (P/T) ratio. In the following, we describe our approaches to obtaining the photopeak efficiency and (P/T) ratio from ^{60}Co source spectra. For this source, the efficiency is traditionally reported for the 1333-keV transition.

We chose the ^{60}Co source both because it is commonly used for such measurements and because it allows efficiencies to be obtained using both the so–called calibrated source (CSM) and sum peak (SPM) methods [25–28]. Each of these two approaches can be applied to spectra generated from a given array in different ways. For both conventional and tracking arrays, two spectra can be created using the signals from the central contacts (CC) of the Ge detectors. One, henceforth referred

to as CCsum, is created by producing spectra for each individual detector and subsequently adding these together. The other, referred to as CCcal below, is a calorimetric spectrum obtained by adding up the energies from all central contacts and histogramming these into one single spectrum. Whichever method is used, it is important to apply the proper corrections when extracting peak areas, taking into account all effects such as: one γ ray removes counts in the other one (in the case of a ^{60}Co source) and/or the effect of having random background γ rays in addition to the γ rays from the source [26, 27]. These considerations are described in sections 2.1 and 2.2.

A third way of obtaining the efficiency at 1333 keV for a ^{60}Co source consists of employing either an additional detector outside the array to trigger on the detection of the coincident 1173-keV transition, or in using an internal detector in the array in the same manner. These methods are described in Sec. 2.3.

While these approaches can be applied to both conventional and tracking arrays, the latter are designed to produce tracked spectra and this requires further processing of the data. The additional factors required to take into account the tracking efficiency are presented in section 3.1.

2.1. The peak areas in a ^{60}Co source spectrum

The CSM relies on a measurement of the observed area of the 1333-keV peak, taking into account a number of corrections, and knowledge of the source strength. The SPM relies on the precise determination of the areas of all three of the 1173-, 1333- and (sum) 2506-keV peaks in the ^{60}Co source spectrum. In either case, the peak areas depend on several factors, including the efficiencies at both 1173 and 1333 keV. In fact, the observed areas of the three peaks in a ^{60}Co source spectrum can be written as:

$$A^{obs}(1173) = S\,\epsilon_p(1173)(1 - C_k(1333)) \times (1 - C_R)(1 - C_s(1173)), \quad (1)$$

$$A^{obs}(1333) = S\,\epsilon_p(1333)(1 - C_k(1173)) \times (1 - C_R)(1 - C_s(1333)), \quad (2)$$

$$A^{obs}(2506) = \frac{1}{N} S\,\epsilon_p(1173)\epsilon_p(1333)C_f(1 - C_R) \times (1 - C_s(1173))(1 - C_s(1333)), \quad (3)$$

(4)

where

$$C_k(e) = \frac{C_o C_f \epsilon_T(e)(1 + C_s(e))}{N}, \quad (5)$$

$$(P/T) \equiv \epsilon_p/\epsilon_T, \quad (6)$$

$$C_R = \frac{\epsilon_R \Delta t}{N}\frac{dR}{dt}, \quad (7)$$

$$S = A_S t L_F. \quad (8)$$

ϵ_T is the total array efficiency, ϵ_p the array photopeak efficiency, and (P/T) is the peak–to-total ratio, all of which are energy dependent. N is the number of crystals in the array with $N \equiv 1$ for the calorimetric CCcal spectra and $N > 1$ for the CCsum spectra. S denotes the total number of γ rays emitted by the source (during the acquisition time t), corrected for any deadtime or loss in efficiency of the system through the live fraction (L_F) [24]. A_S is the source activity and C_f corrects for the angular correlation between the 1173– and 1333–keV lines in the ^{60}Co source [29, 30]. The small corrections for internal conversion and branching ratios for the γ rays from the ^{60}Co source are ignored in the formulas; they are of the order of 0.01%.

To be consistent, one should report the (P/T) ratio at an energy of 1333 keV like the efficiency. However, traditionally, the (P/T) for a ^{60}Co source is reported as

$$(P/T)_{composite} = \frac{A(1173) + A(1333)}{A_{tot}} \quad (9)$$

We shall use this composite (P/T) ratio here as well, but will argue that $A(2506)$ needs to be added to the numerator unless it is tracked data. This ratio can be made from observed areas, $(P/T)^{obs}$, or for the corrected areas of the peaks (see discussion in Sec. 2.2). The composite (P/T) ratio in Eq. 9 can be written as a weighted average of the energy dependent (P/T) values in Eq. 6, using information from a measured response function [30] or spectra gated on the 1173– and 1333–keV lines. For Gammasphere, it is found that

$$(P/T)(1173) = (P/T)_{composite} \times 1.02212 \quad (10)$$

$$(P/T)(1333) = (P/T)_{composite}/1.02212 \quad (11)$$

The value of C_f depends on whether the CCsum or CCcal spectra are used as well as on the distance from the Ge crystals to the source. The nominal value of C_f is found to be 1.1111 at zero degrees [29]. For Gammasphere, taking into account the opening angle of the Ge detectors ($\pm$ 7.5°), the attenuated C_f value is determined to be 1.109 for CCsum [30]. For CCcal spectra in Gammasphere, because the array covers almost 4π, C_f is close to one. For GRETINA, at the nominal distance, the C_f values are specified in Table 1 (see further discussion in Sec. 4.4). Just using the crystal center positions, the C_f values are calculated to be 1.0076 for GRETINA for CCcal spectra; but measured values will be used in the calculations.

Table 1: The angular correlation factors, C_f, used in this work. The values for GRETINA, for the CCcal spectra, are obtained from measurements presented in Sec. 4.4. GRETINA and Gammasphere are abbreviated GS and GT, respectively, in this table.

	C_f(GS)	C_f(GT) (ANL)	C_f(GT) (MSU)
CCsum	1.109	1.107	1.107
CCcal	1.0	1.007	1.013

The combined terms $C_k(e)$ in Eq. 1–2 correct for the fact that one of the γ rays from the ^{60}Co source may hit the detector and remove counts that should belong to the photopeak of the other transition. If only this effect is included, $C_o \equiv 1$ [30]. Setting $C_o > 1$ allows for corrections *beyond* what is already reflected in any decrease of the (P/T) ratio caused by scattered γ rays.

C_R is the correction for random γ rays hitting the detector in addition to photons from the ^{60}Co source. In Eq. 7, $\frac{dR}{dt}$ is the background rate, Δt the coincidence time window and ϵ_R the mean efficiency for total absorption of the random γ rays.

Finally, the C_s coefficient is the probability for a γ ray to scatter out of a crystal, to be detected by other crystals in the array and successfully sum up to the photopeak energy. The coefficient is, per definition, > 0 *only* for the CCsum spectra. Its value can be determined by comparing the counts in the photopeaks of the CCsum and CCcal spectra, taking into account the other correction factors in eqs. 1–2 or, alternatively, from Eq. 20 from Sec. 2.2 below. For tracking arrays this coefficient is significant. On the other hand, for Gammasphere, where the BGO Compton suppressors largely prevent direct scattering between neighboring crystals, the coefficient is smaller.

The concept behind the C_s parameter is also known from composite HPGe detectors, such as Clover detectors, where the energies deposited by a γ ray scattering between crystals are added back and the gain in photopeak counts is measured by the add-back factor F [31]. Treating a tracking array as a single, composite detector, one can also assign an add–back factor F describing the gain in photopeak counts by adding up all crystal energies. The relationship between F and C_s is:

$$C_s = \frac{F-1}{F} \tag{12}$$

The C_s factor allows for the use of the CCsum spectrum to determine the efficiency of tracking arrays, though, not independently of the CCcal spectrum.

2.2. *The efficiencies, true counts and (P/T) ratios*

Eqs. 1–3 indicate how the observed peak areas relate to the actual array efficiencies. Once the peak areas have been correctly determined, efficiencies, true peak areas and peak–to–total ratios can be extracted.

For the summed peak method (SPM), the efficiency is given by:

$$\epsilon_p(1333) = N\left\{\frac{A^{obs}(2506)}{A^{obs}(1173)C_f}\right\} / \left\{1 - C_s(1333) + \frac{A^{obs}(2506)}{A^{obs}(1173)}\frac{C_o(1+C_S(1173))}{N(P/T)(1333)}\right\} \tag{13}$$

On the other hand, for the calibrated source method (CSM), the efficiency is given by:

$$\epsilon_p(1333) = \frac{A^{obs}(1333)}{S(1-C_R)(1-C_s(1333))} + \frac{C_o(1+C_S(1173)A^{obs}(2506)}{NS((P/T)(1173))(1-C_R)(1-C_s(1173))(1-C_s(1333))} \tag{14}$$

Combining eqs. 1–3, we find that the true, corrected counts in the peaks are given by:

$$A^{true}(1173) \equiv S\,\epsilon_p(1173) = \frac{A^{obs}(1173)}{(1-C_k(1333))(1-C_R)(1-C_s(1173))}, \tag{15}$$

$$A^{true}(1333) \equiv S\,\epsilon_p(1333) = \frac{A^{obs}(1333)}{(1-C_k(1173))(1-C_R)(1-C_s(1333))}, \tag{16}$$

$$A^{true}(2506) \equiv S\,\epsilon_p(1173)\epsilon_p(1333)C_f = \frac{A^{obs}(2506)}{(1-C_R)(1-C_s(1173))(1-C_s(1333))}. \tag{17}$$

$$\tag{18}$$

It follows that the true (P/T) ratio for the spectra is:

$$(P/T)^{true} = \frac{A^{true}(1173) + A^{true}(1333) + A^{true}(2506)}{A^{true}_{tot}}, \tag{19}$$

where A^{true}_{tot} is the total number of counts in the spectra up to just past the 2506–keV sum line and is related to the observed counts by:

$$A^{obs}_{tot} = A^{true}_{tot} + \frac{C_s}{(P/T)^{true}}(A^{true}(1173) + A^{true}(1333) + A^{true}(2506)) \tag{20}$$

For CCcal spectra, A^{true}_{tot} is simply A^{obs}_{tot}. Note that, for an ideal 4π array, all the γ rays from a ^{60}Co source will be in the 2506–keV peak in the CCcal spectrum; Eq. 19 remains valid in this case.

For Compton–suppressed arrays, the composite (P/T) ratio is traditionally determined using the CCsum spectrum. This spectrum is most relevant for the spectra used in γ–ray spectroscopy with Compton–suppressed arrays. For tracking arrays, where photons can scatter freely between the crystals, obtaining the (P/T) ratio for the array using the CCsum spectrum is possible, but the additional correction factors mean that the result is less precise.

The proper (P/T) ratio values to use in eqs. 1–3, in order to determine $\epsilon_T = \frac{\epsilon_P}{(P/T)}$ (see Eq. 6), are in fact the $(P/T)^{true}$ ratio from Eq. 19, not the observed values. Since $(P/T)^{true}$ is not known until the efficiency is found from Eq. 13 or Eq. 14, followed by eqs. 15–19, a simple iteration procedure is applied to find the $(P/T)^{true}$ value that reproduces itself.

2.3. *The external trigger method*

A third approach, using the CCcal spectrum, provides another way to measure the efficiency of an array. If a ^{60}Co source is placed at the target position and an external detector is used to detect the 1173–keV line, then the counts in the 1333–keV peak of the CCcal spectrum can be written as:

$$A^{obs}(1333) = A^{obs}_{ext}(1173) \times \epsilon_p(1333)C_f(1-C_R) \tag{21}$$

where $A^{obs}_{ext}(1173)$ is the number of counts seen in the 1173–keV peak in the external detector. Using this method, it should only be necessary to correct for random events in the coincidence time window and for angular correlation effects. It follows that:

$$\epsilon_p(1333) = \frac{A^{obs}(1333)}{A^{obs}_{ext}(1173)C_f(1-C_R)} \quad (22)$$

The external detector could be made part of the tracking array data acquisition system (DAQ). In that case, one can keep track of how many times a 1333–keV line is seen in the tracking array when the channel with the external detector has observed a photopeak absorption of 1173 keV. This ensures that a 1333–keV γ ray has indeed been emitted.

A variation of this method is to identify events in which the 1173–keV transition was detected in one of the array's crystals, and then exclude that specific crystal from the counts contributing to the CCcal spectrum. The exclusion of one crystal from the CCcal spectrum can be taken into account by adding a $\frac{N}{(N-1)}$ correction factor to Eq. 22, where N is the number of crystals.

3. Tracking

The previous sections lay out the procedures for obtaining the array's efficiency at 1333 keV and for measurements of the (P/T) ratio for two types of *untracked* spectra, CCsum and CCcal. These spectra enable direct comparisons between conventional, escape-suppressed and new–generation tracking arrays. However, we are ultimately interested in the sensitivity of the arrays when used in the tracking mode. In the following, both the tracking efficiency and the tracking *deficiency* are considered, and we argue that the latter is an important quantity to evaluate.

3.1. The tracking efficiency

In tracking arrays, the signals from the preamplifiers are digitized into signal traces of a few micro–seconds length at typically 100 MHz sampling. In the decomposition, or pulse shape analysis, traces from the segments of the crystals are analyzed and the interaction positions are inferred from fits that compare these traces with a basis data set. Tracking algorithms are then used to reconstruct the trajectories of the incident γ rays in order to determine their energy and direction. To accomplish this, the algorithms must group interaction points into those likely originating from a given γ ray and establish their scattering sequence (or order). Tracking algorithms can be divided into two classes: those based on back tracking [5] and those based on clustering and forward tracking [6]. The latter approach is used in this work.

For photon energies of interest (tens of keV to 20 MeV), the main physical processes that occur when a photon interacts in germanium are Compton scattering, Rayleigh scattering, pair creation and photo absorption. Since Compton scattering is the dominant process between 150 keV and 10 MeV, all current tracking algorithms are based on the properties of this interaction process.

How closely the interaction points follow the Compton scattering formula

$$E^{'}_{\gamma} = \frac{0.511}{1 + \frac{0.511}{E_{\gamma}} - cos(\theta)} \quad (23)$$

is evaluated by the Figure of Merit (FOM)

$$FOM = \sum_i \frac{\sqrt{(\sum_i(\theta^{theo}_i - \theta^{obs}_i)^2)}}{n_i - 1}; n_i > 1 \quad (24)$$

where θ^{obs}_i are the observed scattering angles and θ^{theo}_i are the angles (in radians) from the Compton scattering formula, based on the energy deposited, E_{γ}- $E^{'}_{\gamma}$, at the interaction points and n_i is the number of interaction points. If the angle θ becomes unphysical, based on the scattering energy, a penalty in the FOM sum, Eq. 24, is added. For photons with more than one interaction point, typically upper limits on the FOM for a γ ray to be considered "good" are in the range from zero up to $0.6 < \mathrm{FOM}_{max} < 0.8$. Gamma rays that have been assigned higher FOM by the tracking algorithm are rejected. An interaction point that is not clustered with other ones (i.e., when $n_i \equiv 1$) is referred to as a *single–interaction point* γ ray. Such photons cannot be tracked and are assigned a FOM of zero, unless they are located beyond their range in the crystals, in which case they are assigned a FOM value of 1.85 (see Appendix B).

With a calibrated ^{60}Co source, the number of 1333–keV γ rays absorbed in the tracking array should be $S\,\epsilon_p(1333)$ (see eqs. 1–5). Thus if, in the tracked spectrum, $A_T(1333)$ counts are measured instead, the tracking efficiency for a given FOM cut is:

$$\epsilon_{track} = \frac{A_T(1333)}{S\,\epsilon_p(1333)} \quad (25)$$

If an uncalibrated ^{60}Co source is used, this ratio can still be found using Eq. 16 as

$$\epsilon_{track} = \frac{A_T(1333)}{\frac{A^{obs}(1333)}{(1-C_k(1173))(1-C_R)(1-C_s)}} \equiv \frac{A_T(1333)}{A^{true}(1333)} \quad (26)$$

where $A^{true}(1333)$ is the true counts in the CCcal spectrum defined in Eq. 16. For tracked data, the experimental photopeak efficiency is the array efficiency, eqs. 13 and 14, multiplied by this tracking efficiency. These are the efficiencies that we obtain below and that we present in Fig. 6.

For tracked spectra, the area of the 2506–keV peak should not be included in the (P/T) ratio as it should ideally be absent since such events should have been tracked and resolved into two γ rays of 1173 and 1333 keV. Thus, we suggest that the proper (P/T) ratio to be used and reported for *tracked* spectra is simply:

$$(P/T)^{tracked} = \frac{A_T(1173) + A_T(1333)}{A_{tot}}, \quad (27)$$

where A_{tot} is the number of counts from some lower–energy limit up to just past the 2506–keV line in the tracked spectra. Any counts in the 2506–keV peak should be considered to belong to the total part, A_{tot}. In this paper, the (P/T) ratio is measured with background subtraction under the 1173–, 1333– and 2506–keV lines.

We propose that a measure of the tracking deficiency for a ^{60}Co source is

$$TrD = \frac{A_T(2506)}{A_T(1173) + A_T(1333)}, \quad (28)$$

where the areas A_T are from the tracked spectra (for a given FOM range acceptance). Tracking can, for real data, never completely remove the summed 2506 peak and, if TrD is too large, there will be artificially summed peaks in the actual tracked spectra. Getting a high tracked efficiency, (P/T) ratio and yet a small tracking deficiency requires compromises in the values of the tracking parameters as will be discussed in the following. For a ^{60}Co source, the tracking deficiency as a function of FOM cuts has been found to be small (less than 1 % for the size of the tracking array examined in this work). The concept of the tracking deficiency can be generalized for any source as:

$$TrD = \frac{\sum_i \sum_j A_T(E_i + E_j) + \sum_i \sum_j \sum_k A_T(E_i + E_j + E_k) \ldots}{\sum_i A_T(E_i)}, \quad (29)$$

where the sum is over peak areas of γ rays in coincidence and where $i < j < k$.

3.2. The clustering angle (α)

One of the most critical parameters in tracking algorithms is the clustering angle used to associate a set of interaction points with (potential) γ rays. The γ rays reconstructed in this manner may later be re-clustered (split and combined) depending on their FOM values. Even though the tracking algorithm has the ability to split and combine clusters, the initial clustering angle that is used has a strong influence on the quality of tracked spectra.

The minimum clustering angle required for good tracking can be estimated by examining the spread of angles between interaction points for a ^{60}Co source in the tracking array, as shown in Fig. 1. This curve reveals the minimum clustering angle to be used if a given probability for collecting all the interaction points for the γ rays emitted by a ^{60}Co source is to be reached.

Figure 2, which is an integral of the curve in Fig. 1, suggests that the clustering angle should be no less than around $11^\circ - 12^\circ$ in order to collect at least 90% of the interaction points created in the detectors for a ^{60}Co source. Although it is tempting to increase the clustering angle to achieve increasingly better tracked spectra, this cannot be done for in–beam data with high γ-ray multiplicity, as this would result in the mistaken clustering of separate γ rays. The probability for at least two γ rays

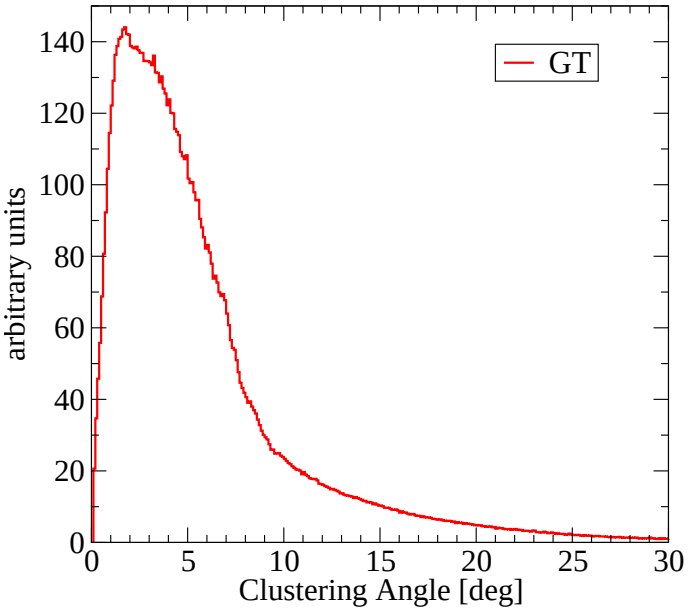

Figure 1: The measured angle spread of interaction points for the γ rays from a ^{60}Co source in the GRETINA tracking array based on the decomposed (pulse shape analyzed) data from the spectrometer.

in a cascade to be wrongly "double-clustered", P_{dc}, is approximately:

$$P_{dc} \approx \epsilon_T \left(1 - \prod_{i=1}^{m-1} \left(1 - \frac{i\epsilon_T}{n}\right)\right) \quad (30)$$

$$n = \frac{2}{(1 - cos(\alpha/2))} \quad (31)$$

where α is the clustering angle, ϵ_T the total array efficiency and m is the multiplicity of the γ–ray cascade from a source or from in–beam reaction residues; n is the number of clusters for the clustering angle α[1]. If one wants to keep this double–clustering probability below 1% , 5% or 10%, for a given clustering angle and calculated for the full GRETA array with 120 crystals, the maximum γ–ray multiplicity, m, that can be accepted is given in Table 2. Thus, for typical heavy–ion induced fusion reactions producing high multiplicity γ-ray cascades, the choice of clustering angle is a compromise between tracking widely–scattered γ rays and reducing the number of false double clusters.

The above discussion provides some guidance as to the value of the clustering angle to use for a given data set. One could try to optimize the α angle by maximizing at the product $[P \times P/B]$ for a representative line in the spectra. Here, P is the area of the peak and B is the background level under the same peak. This measure optimizes both the efficiency and the (P/T) ratio of the tracked spectra, thus finding the best compromise for the clustering angle.

[1] If ϵ_T=1 and α=12° (n = 365), eqs. 30 and 31 solve the well known 'birthday problem'; *i.e.*, how many people have to be in a room before there is a 50% chance that two have the same birthday.

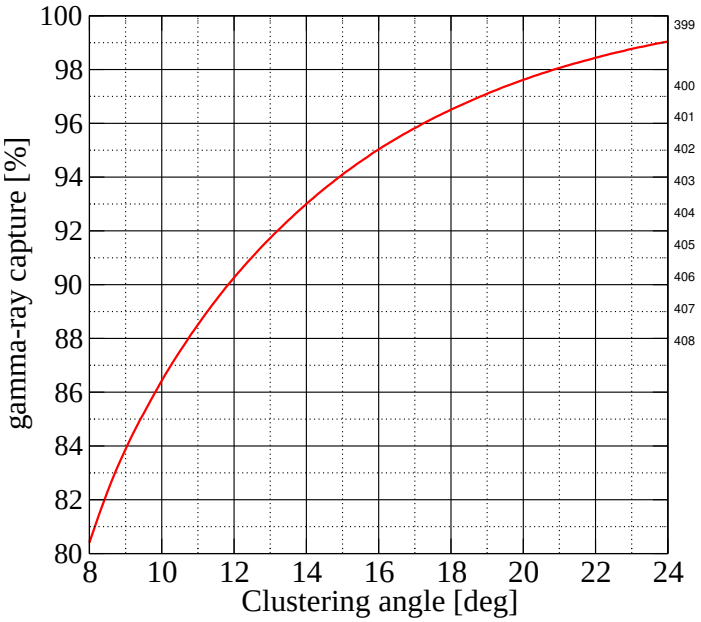

Figure 2: The minimum clustering angle needed to group interaction points into a γ ray for GRETINA with the resulting clustering efficiency given on the y axis. These curves are obtained by a simple integration of the curve displayed in Fig. 1.

4. Results and comparisons

As mentioned in the introduction, a suitable approach to test the formulas and procedures discussed above is to first apply these to data from Gammasphere. The results are presented in section 4.1. The array efficiency is extracted for GRETINA in section 4.2. Sec. 4.4 presents tracking angular correlation results while Sec. 4.5 compares the ^{60}Co spectra obtained in the Gammasphere and GRETINA arrays. Finally, Sec. 4.6 compares the (P/T) versus efficiency data for the arrays.

Table 2: The maximum multiplicity, m, that can be accepted for a given clustering angle, α, in order to keep the double clustering probability, P_{dc}, in the full GRETA array below the limits of 1, 5 or 10% for a ^{60}Co source. For GRETA, the photopeak efficiency has been extrapolated to be 34% (see Sec. 4.2) and a (P/T) ratio of the order of 0.6 is expected. Thus, the total array efficiency (see Eq. 30), is expected to be about 62%, the value used to produce this table.

P_{dc} / α[deg]	<1%	<5%	<10%
	m	m	m
8	7	15	22
10	5	12	17
12	4	10	14
14	4	8	12
16	3	7	11
18	3	7	10
20	3	6	9

4.1. The efficiency of Gammasphere

Table 3 presents measurements of the efficiency for Gammasphere. Two calibrated ^{60}Co sources were used, one isotopically pure and one mixed. The mixed–isotope source was weak and calibrated, containing ^{60}Co, ^{137}Cs and small traces of other radioisotopes. With these data, a good test of the random correction terms in the efficiency formulas is possible. With two sources, two methods and both the CCsum and CCcal spectra, there are eight measurements and the results are compared in Table 3.

Table 3: Measured array efficiencies for Gammasphere, scaled to 100 detectors, using two methods, two spectra and two sources. Traditionally, the (P/T) value derived from the CCsum spectrum is reported as the ratio for the Gammasphere array because it is the relevant ratio for spectra where gates are placed on γ rays. The deadtimes used in the CSM analysis are discussed in Appendix A.1.

	SPM	CSM
CCsum spectrum, C_s=0.040(5)		
ϵ_P(mixed)	8.6(9)%	8.0(3)%
ϵ_P(pure)	8.8(2)%	7.6(8)%
$(P/T)^{obs}$	0.471(5)	0.471(5)
$(P/T)^{true}$	0.514(5)	0.492(5)
C_o	1.10(5)	1.10(5)
CCcal spectrum, C_s=0		
ϵ_P(mixed)	7.9(2)%	8.3(3)%
ϵ_P(pure)	7.9(2)%	7.8(4)%
$(P/T)^{obs}$	0.460(5)	0.460(5)
$(P/T)^{true}$	0.537(5)	0.540(5)
C_o	1.10(5)	1.10(5)

For the CSM method, in calculating the live fraction L_F (see Eq. 8) for Gammasphere, we take into account various deadtimes of the system as well as other inefficiencies of the DAQ readout system, see Appendix A.1. Using all the methods and sources, with proper corrections, the efficiency of Gammasphere is determined to be 8.2(1)% with a (P/T) ratio of 0.52 using the weighted sum of all the results. The (P/T) ratio and efficiency are somewhat lower than those reported in Ref. [30] because the light collection efficiency in the BGO Compton Suppressors has deteriorated somewhat over time. In 2007, the efficiency of Gammasphere was measured to be 8.9(1) with a (P/T) ratio of 0.54, using slightly less accurate formulas compared to those presented in this work. For the comparison with the GRETINA tracking array, the 2007 optimal Gammasphere performance regarding the (P/T) will be used as the standard.

4.2. The efficiency of GRETINA at ANL

At the time of these measurements, GRETINA consisted of 28 crystals. The array efficiency at 1333 keV was measured with two sources, as was the case with Gammasphere (see Sec. 4.1). The clustering angle for tracking was set to 20°. The results are presented in Table 4. As discussed in Sec. 3, the tracking efficiency is obtained by comparing the number of counts in the photopeaks of the tracked spectrum with the corrected counts

from Eq. 16. The tracking efficiency is given for tracked spectra without FOM cuts. The subscripts *wsi* and *nsi* refer to spectra that include and exclude single interactions in the tracking, respectively. An experimentally measured value of $C_f = 1.00645$ was used (see Sec. 4.4).

Table 4: Measured array efficiencies for GRETINA with 28 crystals at the nominal distance of 18.5 cm at ANL. The deadtimes used in the CSM analysis are discussed in Appendix A.2. See text for details.

	SPM cal	CSM cal	SPM sum
ϵ_P(mixed)	6.02(15)%	6.24(18)%	-
ϵ_P(pure)	6.40(6)%	6.0(6)%	6.5(6)%
$(P/T)^{obs}$	0.321(3)	0.321(3)	0.192(2)
$(P/T)^{true}$	0.386(4)	0.382(3)	0.363(11)
$\epsilon_{track,nsi}$	91(1)%	92(2)%	92(1)%
$\epsilon_{track,wsi}$	93(1)%	94(2)%	93(1)%
C_s	0	0	0.293(5)
C_0	1.02(2)	1.02(2)	1.02(2)

The efficiency was also measured with an external detector (as described in section 2.2) to be 6.39(17)%. The errors in Table 4 take into account the full error propagation for all the variables in eqs. 13 and 14 above.

The photopeak efficiency for GRETINA is determined to be 6.45(4)%, using a weighted mean of the values in Table 4, combined with the external detector measurement, and the true (P/T) ratio is measured to be 0.38.

From these results, the expected efficiency of the full GRETA spectrometer can be estimated. The full 4π array will have 120 crystals; the occupancy of GRETINA for the current measurement was thus 28/120=23.3%. The efficiency per crystal is determined to be 0.229(2)%. Hence, for a 4π array, an efficiency of at least 27.4(2)% would be expected using simple scaling. This is, however, only a lower limit since the more crystals fill the array, the less 'open' surface there is where γ rays can escape and the scaling should, therefore, not be linear. Using the AGATA–GEANT4 code [32] (with an uncertainty of 10% in the simulations) for this scaling yields a 4π array photopeak efficiency of 34(4)%, or about 4 times that of Gammasphere.

4.3. The efficiency of GRETINA at MSU

At MSU, the GRETINA array was configured slightly more compact (see Sec. 5) and the analysis of the data from the MSU setup is presented in Table 5. A weak, calibrated ^{60}Co source was used, thus, all spectra were background subtracted.

4.4. Angular correlations in tracking arrays

The fact that tracking algorithms cluster together interactions within a given solid angle impacts angular correlation measurements from tracked data. The extent of this impact is illustrated by extracting angular correlation information for the γ rays from a ^{60}Co source. The procedure is as follows: for each event where one 1173– and one 1333–keV γ ray are present, the angle between the first interaction points for the two photons is found and is histogrammed, herewith revealing the set of *correlated* events.

Table 5: Measured array efficiencies for GRETINA at MSU with 28 crystals at the nominal distance of 18.5 cm from the target position. See text for details.

	SPM cal	SPM sum
ϵ_P(pure)	6.30(14)%	6.58(44)%
$(P/T)^{obs}$	0.366(5)	0.215(3)
$(P/T)^{true}$	0.434(5)	0.428(20)
$\epsilon_{track,nsi}$	89(1)%	89(3)%
$\epsilon_{track,wsi}$	92(1)%	93(3)%
C_s	0	0.316(5)
C_0	1.02(2)	1.02(2)

This event is also stored and used when the next coincidence event is encountered to construct angles between *uncorrelated* first interaction points from pairs of γ rays originating from events measured at different times. The ratio of the spectrum of correlated angles to that of uncorrelated ones reveals the angular correlation and is presented in Fig. 3 for GRETINA, while using a clustering angle of 10°. Conveniently, the uncorrelated spectrum also allows us to experimentally determine the C_f value discussed in Sec. 2.1. The angular correlation function [29], $\omega(\theta) = 1 + 0.102041P_2(cos\theta) + 0.00907P_4(cos\theta)$, is simply weighted with the normalized uncorrelated spectrum.

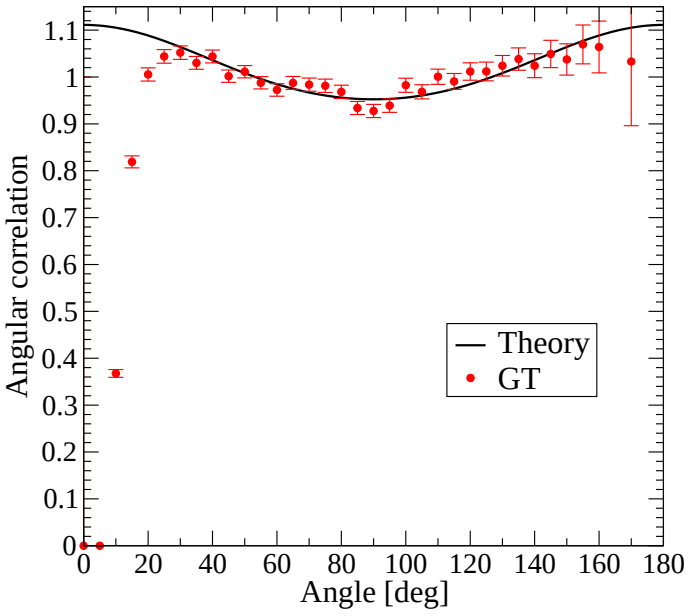

Figure 3: Angular correlation extracted from tracked GRETINA (GT) data for a ^{60}Co source using a clustering angle of 10°. For the tracking, a FOM acceptance from zero to 0.8 was used and the theoretical spectrum is shown without any attenuation. See text for details.

The drop at small angles in Fig. 3 comes from the fact that, if two γ rays are within the pre–determined clustering angle, they will (using current tracking codes) mostly be added up rather

than be recognized as individual photons (see the tracking deficiency discussion in Sec. 2.2). As can be seen in Fig. 3, the *effective* clustering angle is slightly larger than the 10°specified for the tracking because two nearby γ rays may have *some* interaction points that are within the clustering angle.

The tracking arrays offer an angular resolution of $1° - 2°$. If needed, the $\gamma - \gamma$ angular correlation can be extended towards lower angles using a "mix before track" method developed within the AGATA collaboration [33].

4.5. Comparing ^{60}Co source spectra

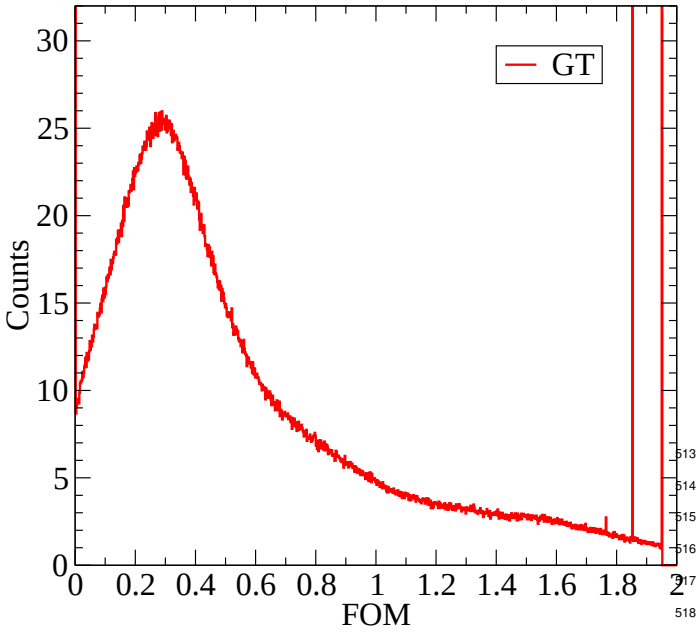

Figure 4: The FOM spectrum for GRETINA for a ^{60}Co source. The single–interaction point γ rays that occurred too deep in the crystals are marked with a FOM≡1.85 rather than zero. Overflows are marked with at FOM of 2.0. See text for details.

Figure 4 provides the FOM distributions (see Sec. 3.1) for tracked γ rays obtained from the GRETINA spectrometer with a ^{60}Co source. In GRETINA, ~7% of the γ rays are assigned FOM=0 by the tracking algorithm and ~8% are single interactions happening too deep into the Ge crystal for this to be probable (see Appendix B). Thus, the latter events are marked with a FOM=1.85, so that they can be rejected in the ensuing sorting.

Figure 5 compares ^{60}Co source spectra from GRETINA at ANL, with and without including single interaction γ rays, and a spectrum from Gammasphere. A FOM cut of 0–0.64 for GRETINA was applied. This particular FOM cut was selected so that 70% of the γ rays are accepted in GRETINA (see Fig. 4). The spectra are normalized such that the same number of counts are present in the photopeaks and no background subtraction has been applied.

In all cases, the (P/T) ratio was determined using a low–energy

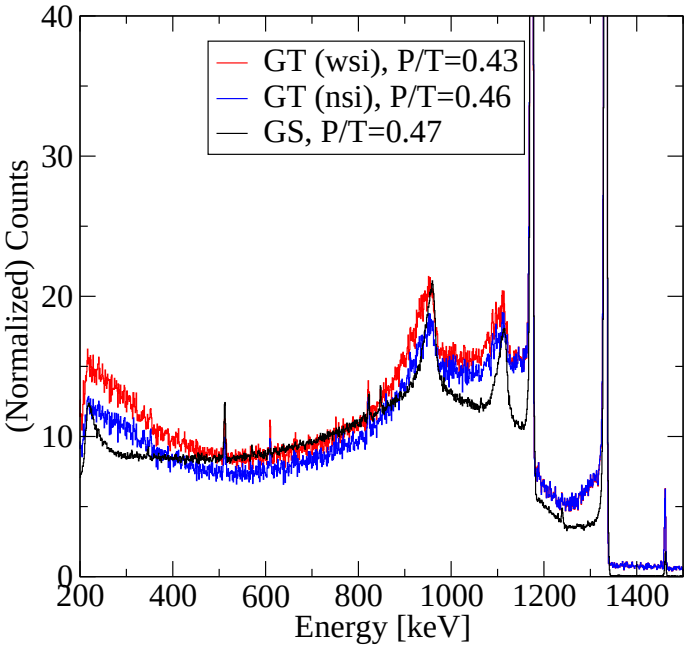

Figure 5: Comparison of spectra from ^{60}Co from GRETINA (GT), with and without single interactions at ANL, and Gammasphere (GS). In all cases, the spectra have been normalized to have the same number of counts in the photopeaks.

bound of 200 keV because Gammasphere was equipped with Ta/Cu absorbers which affect spectra below this energy. At the time the data was recorded, GRETINA had Ta absorbers in front of the seven modules. Hence, a lower bound of 200 keV was applied to all the tracked spectra and provides for a fair comparison of the measured (P/T) ratios.

4.6. Comparing the (P/T) ratios versus the efficiency curves for GRETINA

The (P/T) ratio vs. photopeak efficiency curves for GRETINA can be found in Figs. 6 and 8, for clustering angles of 20° and 10°, respectively. The clustering angle is typically chosen between these limits, depending on the γ–ray multiplicity (see discussion in Sec. 3.2). The two curves in the figures demonstrate the effect of *including* (wsi) and *excluding* (nsi) photons with a single–interaction points. The curves are provided for FOM cuts of 0–0.2, 0.4 . . . 2.0 (from left to right) where a FOM cut of 0–2.0 is equivalent to no cut at all.

5. Discussion

As can be seen in Figs. 6–8, in GRETINA there is not much difference between the nsi and wsi curves in terms of efficiency (see also Table 4). Indeed, when extracting the probability for a photopeak event as a function of the number of interaction points, after tracking, it is clear that there are many single–interaction points that do not contribute to the photopeaks for

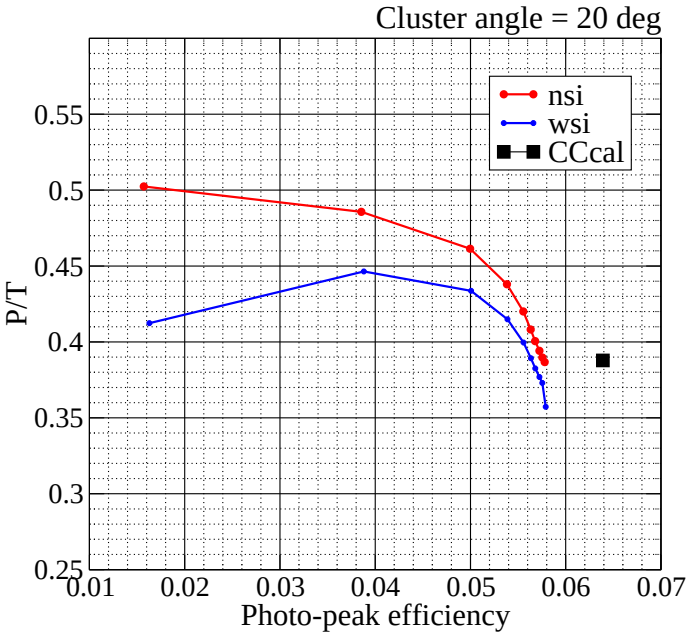

Figure 6: The (P/T) ratio vs. photopeak efficiency curves for GRETINA (ANL setup), with 7 closed-packed modules, when a clustering angle of 20° is used. The lower curve includes single interactions (wsi) and the upper curve is obtained without these interactions (nsi).

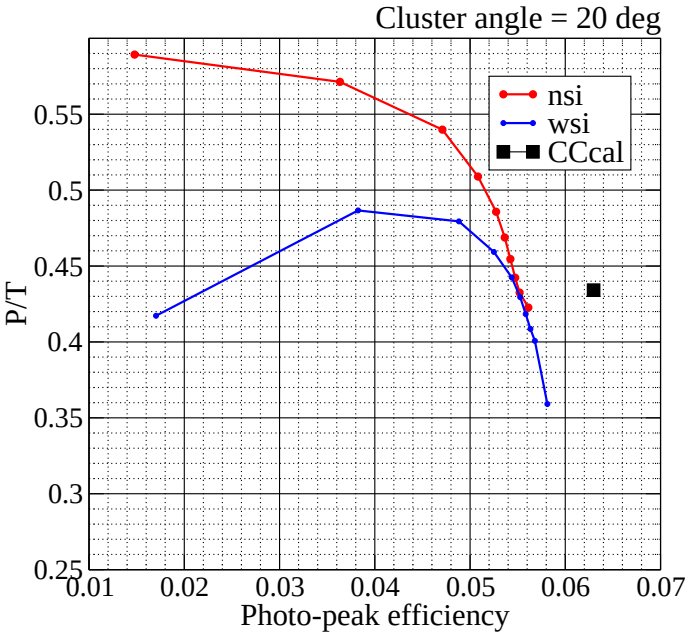

Figure 7: The (P/T) ratio vs. photopeak efficiency curves for GRETINA (MSU setup), with 7 closed-packed modules, when a clustering angle of 20° is used. The lower curve includes single interactions (wsi) and the upper curve is obtained without these interactions (nsi).

a ^{60}Co source: this is shown in Table 6. Only 2% of the photopeaks contain single interactions. Data from GEANT4 simulations suggest that ~10% of the photopeaks ought to be from single–interaction events. The data from the GEANT4 simulations were smeared to have the same position and energy uncertainty as data from the tracking array [7, 34] and a packing parameter of 6 mm was used (*i.e.*, GEANT4 interactions within 6 mm were combined into one interaction). It was not possible to find realistic packing parameters that could fully reproduce the data in Table 6.

Table 6: Distribution of the number of interaction points in the tracked *photopeak* γ rays for a ^{60}Co source in GRETINA and those obtained from a GEANT4 simulation with the parameters outlined in the text.

number of interaction points	GRETINA photopeak	GEANT4 photopeak
1	2%	10%
2	21%	27%
3	35%	31%
4	24%	21%
5	13%	10%
6	4%	3%
7	1%	1%

In the GRETINA decomposition, the fits of the segment traces [14] allow for more than one interaction per segment. One might suspect that the fitting function sometimes places two interaction points in a segment where there should have been only one – because it results in a better χ^2 in the fitting procedure. Hence, it is possible that, in general, the GRETINA decomposition overestimates the number of interaction points associated with a photon.

Both the array efficiency and, especially, the tracking efficiency depend on the degree to which a tracking array is compact, *i.e.*, how closely the crystals are packed in the array. A measure of the compactness of a tracking array may be obtained as follows: for each crystal, one can count how many of the sides of the crystal have a near (contact) neighbor, add up the numbers for the individual crystals and divide by the number of crystals times six (*i.e*, the total number of sides). With 28 crystals during the campaign at ANL, a compactness value of 63% is obtained (see section 4.2). In an earlier setup at MSU, a compactness of 70% was achieved (see section 4.3). The detailed effect of compactness on the tracking performance is under investigation [35].

Figure 9 presents the absolute efficiency for Gammasphere and GRETINA as a function of γ–ray energy. The GRETINA data were tracked with a clustering angle of 20° and a FOM cut of 0–0.8. It was possible to determine the efficiency only up to ~3 MeV because of the energy range selected for the central contact during the measurements. The Gammasphere curve is given for the standard 100 detectors, as well as when scaled to the same occupancy as GRETINA; *i.e.*, 28/120.

Finally, using a ^{60}Co source, we suggest that it is possible to numerically compare Gammasphere and GRETINA by evaluating a figure of merit defined as $[\epsilon_p \times (P/T)]$, and using the optimum place on the (P/T) ratio vs photopeak efficiency curves presented in Figs. 6–8. Using spectra from the GRETINA tracking

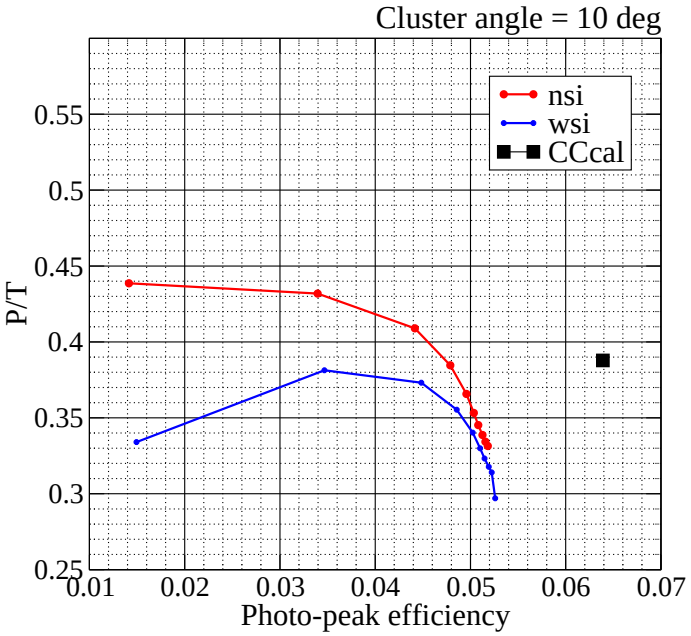

Figure 8: Same as Fig. 6; but now using a clustering angle of 10°.

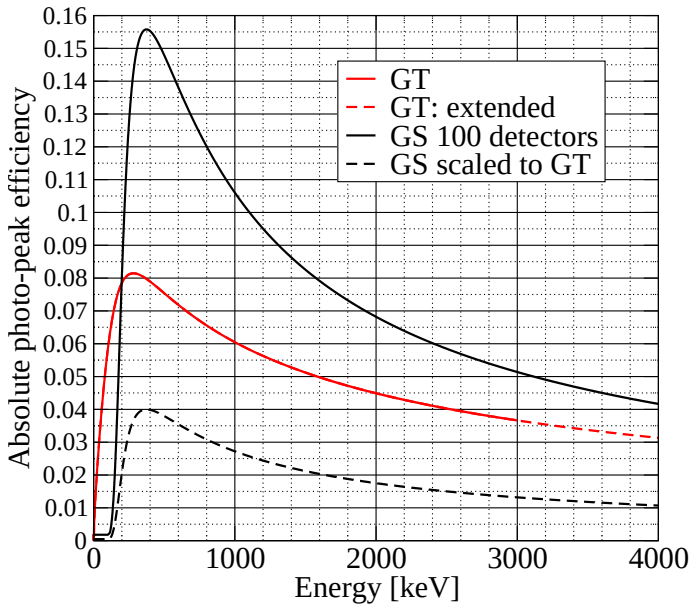

Figure 9: The absolute efficiency of Gammasphere and GRETINA (with 28 crystals) as a function of energy.

array with a clustering angle of 20°, and excluding (or including) the single–interaction points, the results are given in the second (third) column of Table 7.

If one takes $[\epsilon_p \times (P/T)]$ as the measure, with 100 modules in Gammasphere and 28 crystals in GRETINA, Gammasphere is about twice as sensitive as GRETINA. However, when scaled to an occupancy of 23.3% (*i.e.*, that of GRETINA), GRETINA is approximately twice as sensitive as Gammasphere (see Table 8). If a figure of merit of $[\epsilon \times (P/T)]^2$ was used (Table 7), which would be more relevant for gated coincidence spectra [23], GRETINA would be about four times as sensitive as Gammasphere. The $[\epsilon_p \times (P/T)]$ figure of merit used here is, of course, only one of many possible measures. In many in–beam experiments, the superior angular resolution and, thus, Doppler correction offered by the tracking arrays will be of much more importance [36].

Table 7: Numerical comparison of Gammasphere and GRETINA using the figure of merit measure of $[\epsilon_p \times (P/T)]$, including single–interaction γ rays (wsi) and excluding them (nsi). See text for details.

	$[\epsilon_p \times (P/T)]$	
device	(nsi)	(wsi)
Gammasphere	0.0427	0.0427
GRETINA	0.0236	0.0223

6. Conclusions and outlook

We have found that, generally speaking, tracking γ detector arrays are more challenging to characterize than the Compton–suppressed γ–ray spectrometers of the previous generation.

Table 8: Comparison of Gammasphere and GRETINA using the figure of merit measures of '$[\epsilon_p \times (P/T)]$' and '$[\epsilon_p \times (P/T)]^2$' and where Gammasphere data have been scaled to have the same occupancy as GRETINA. The (nsi) results exclude single interactions and the (wsi) results include them. See text for details.

	$[\epsilon_p \times (P/T)]$		$[\epsilon_p \times (P/T)]^2$	
device	s(nsi)	s(wsi)	s(nsi)	s(wsi)
Gammasphere	0.0110	0.0110	$1.21\ 10^{-4}$	$1.21\ 10^{-4}$
GRETINA	0.0236	0.0223	$5.57\ 10^{-4}$	$4.97\ 10^{-4}$

However, based on current extrapolations to a full 4π array, they will provide superior performance mainly due to the large HPGe coverage while maintaining a good (P/T) ratio. Possible improvements in electronics, signal–decomposition and tracking algorithms could translate into a better (P/T) ratio and further enhance their potential.

In this work, an attempt was made to provide a formalism to determine the array photopeak efficiencies, tracking efficiencies and true peak–to–total ratios. Some guidelines regarding clustering angles to be used in the γ–ray tracking algorithm have also been proposed.

Throughout this work, a ^{60}Co source was used to characterize the arrays. Many optimizations of the tracking parameters will remove low–energy γ rays in the ^{60}Co spectra and, thus, *appear* to improve the peak–to–total ratio. However, further analysis often reveals that the photopeaks associated with low energies are much reduced as well. We suggest that a ^{166}Ho source is a better choice to use for the characterization of tracked spectra. This source has transitions that are in coincidence with each other and this will allow to improve the tracking algorithms and optimize their parameters. In addition, it has low-energy lines that a ^{60}Co source lacks and it has a strong branch with four γ

rays in coincidence with respective energies of: 711.7, 810.3, 184.4 and 80.6 keV. Other γ rays in coincidence can be used as well. Work is in progress on improving the tracking of data from the GRETINA spectrometer using this source [37].

We have developed software that can translate AGATA data into data in the GRETINA data format (*i.e.*, data containing the interaction point coordinates, energies and timestamps of the γ–ray interactions in the crystals). This would allow for a direct comparison of the performance of the two tracking arrays. Unfortunately, results of an analysis of AGATA data will be published elsewhere [38].

7. Acknowledgments

This material is based upon work supported by the U.S. Department of Energy, Office of Science, Office of Nuclear Physics, under contract number DE-AC02-06CH11357. This research used resources of the ANL's ATLAS facility, which is a DOE Office of Science User Facility. LBNL is supported by the U.S. Department of Energy under Contract No. DE-AC02-05CHI1231 and L. Riley acknowledges support from NSF through grant no. PHY–1303480. This work was also supported by the French National Center of Research, CNRS. D. R. was partially supported by the P2IO Excellence Laboratory. We acknowledge valuable discussions with J. Ljunvall and A. Lopez–Martens.

Appendix A. Deadtime and random rates

If calibrated sources are used to determine the efficiencies of the spectrometers, the deadtimes of the DAQ systems need to be determined. This, of course, also holds if the array is used to determine absolute cross sections.

Appendix A.1. Deadtimes in Gammasphere

In the analog Gammasphere data acquisition system (DAQ), there are two deadtimes. The first is in the the pre–trigger cir-cuitry and is about 1-2 μs. The second deadtime is in the read-out system and is about 19-21 μs depending on the setup. The total DAQ live fraction is taken to be the product of the resulting live fractions. The fact that the analog DAQ stops, for the order of a minute, every time the analog Gammasphere event builder is reset must also be taken into account, herewith resulting in an additional deadtime. This deadtime can be found by inspection of the rate spectra.

The formulas of Ref. [24] were used to calculate the live fractions. The rates in Gammasphere for the the mixed and pure sources were 1.47– and 11.0 kHz, respectively and the live fractions were found to be 0.967 and 0.711, see Table 3. The C_R values for the mixed source are determined to be $26(6)10^{-6}$ and $31(7)10^{-8}$ for the CCcal and CCsum spectra, respectively. For the pure source a value of zero was used.

Appendix A.2. Deadtimes in tracking arrays

Both GRETINA and digital Gammasphere (DGS) have DAQ systems that, as opposed to the analog Gammasphere DAQ system, only have channel deadtimes. Thus, unlike analog Gammasphere, the DAQs for GRETINA and DGS are never totally blocked at any given time, but the overall efficiency is, however, reduced by the unavailability of the channels that are busy (*i.e.*, dead). Using the CSM with the CCcal spectrum, it is mathematically possible to take this into account in Eq. 8, through the L_F factor – even though, in this case, L_F reflects a reduction in efficiency rather than a traditional live fraction of the DAQ. For the CCcal spectrum, the channel live fraction is also the overall array live fraction. However, for the CCsum as well as tracked spectra, the overall array live fraction will be different and will depend on, among other things, the γ–ray multiplicity.

The rate in GRETINA was 3.49 kHz when the weak mixed source was placed at the target position. The channel deadtime was measured to be 22 µs. To be able to handle the rate in GRETINA caused by the 'pure' source, the DAQ was pulsed on and off with an on fraction of 8.92(8)%. The average rate was observed to be 445 Hz, so the actual rate, while the GRETINA DAQ was on, was therefore 5.00 kHz. It follows that the per–crystal counting rates for the two sources were 125 Hz and 179 Hz, resulting in effective live fractions of 0.997 and 0.996, respectively, for the mixed and 'pure' source. Thus, for both sources, the effect of deadtime is negligible. The random rates for the mixed source resulted in $C_R = 25(5)10^{-6}$ and $89(17)10^{-8}$ for the CCcal and CCsum spectra, respectively. For the pure source the C_R value was set to zero.

Appendix B. Range of γ rays in Ge

Photons penetrating a Ge crystal are absorbed with a probability of

$$p(z) = 1 - e^{-(\mu/\rho)\rho z} \tag{B.1}$$

where z is the depth in the crystal from the front face, ρ the density of Ge and (μ/ρ) the mass attenuation coefficient for Ge which depends on the energy of the photon and are tabulated in Ref. [39]. One can, for a given energy of a γ ray, determine the depth in the crystal, $z_{85\%}$, where the γ ray has been fully absorbed with a 85% probability. Fig. B.10 shows the $z_{85\%}$ range values for energies relevant for γ–ray spectroscopy. These range values are used in the tracking procedure to mark (with a FOM of 1.85) single–interaction γ rays that have less than a 15% probability for having interacted at the z range determined by the decomposition and tracking algorithms.

References

[1] P. J. Nolan, F. A. Beck, and D. B. Fossan, Annu. Rev. Nucl. Sci., 45 (1994) 561.
[2] J. Eberth and J. Simpson, Progress in Particle and Nuclear Physics, 60 (2008) 283.

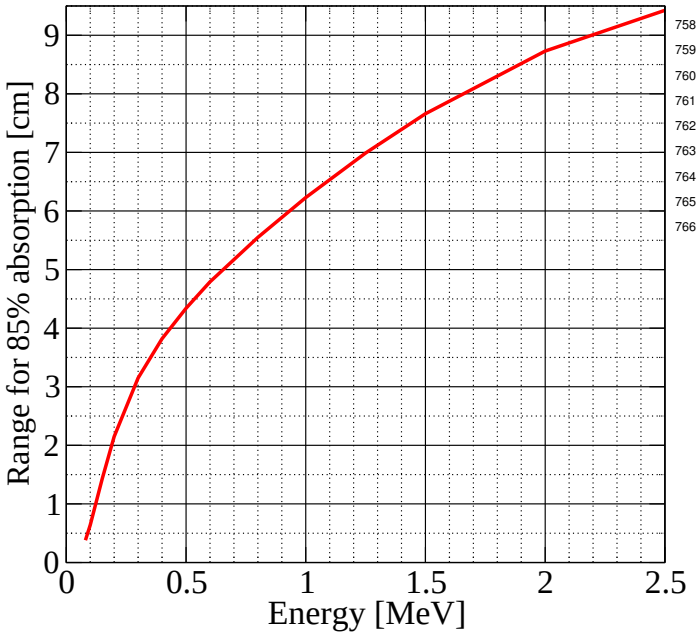

Figure B.10: The depth in a Ge crystal at which a γ ray has been absorbed with a 85% probability. See text for details.

[3] I. Y. Lee, M. A. Deleplanque, and K. Vetter, Rep. Prog. Phys., 66 (2003) 1095.

[4] M. A. Deleplanque, et al., Nucl.Instrum.Methods Phys.Res., A430 (1999) 292.

[5] J. van der Marel and B. Cederwall, Nucl. Instr. Meth. A, 437 (1999) 538 – 551.

[6] G. J. Schmid, et al., Nucl. Instr. Meth. A, 430 (1999) 69 – 83.

[7] D. Bazzacco, Development of gamma-ray tracking detectors, EU TMR network project, unpublished code.

[8] A. Lopez-Martens, et al., Nucl. Instr. Meth. A, 533 (2004) 454 – 466.

[9] F. Didierjean, G. Duchêne, and A. Lopez-Martens, Nucl. Instr. Meth. A, 615 (2010) 188 – 200.

[10] J. Simpson, Z. Phys., A358 (1997) 139.

[11] I–Y. Lee, Nucl. Phys., A520 (1990) 641c.

[12] R. Janssens and F. Stephens, Nucl. Phys. News Int., 6 (1996) 9.

[13] S. Akkoyun, et al., Nucl. Instr. Meth. A, 668 (2012) 26 – 58.

[14] S. Paschalis, et al., Nucl. Instr. Meth. A, 709 (2013) 44 – 55.

[15] I-Yang Lee and J. Simpson, Nulcear Physics News, 20 (2010) 23.

[16] S. Galès, Nucl. Phy., A834 (2010) 717c.

[17] A. Andrighettoa, et al., Nucl. Phy., A834 (2010) 754c.

[18] URL http://www.ganil-spiral2.eu/.

[19] H. H. Gutbord, Nucl. Phy., A752 (2005) 457.

[20] G. Savard, et al., Hyperfine Interactions, 199 (2011) 301–309.

[21] URL http://www.nscl.msu.edu/.

[22] E. S. Reich, Nature, 477 (2010) 15.

[23] D. C. Radford, Proceedings of the International Seminar on the Frontier of Nuclear Spectroscopy, Kyoto, Japan, World Scientific (1992).

[24] G. F. Knoll, Radiation Detection and Measurement, New York : Wiley (2000).

[25] G.A. Brinkman and A.H.W. Aten and J. Veenboer, Appl. Rad. Isot, 14 (1963) 153.

[26] J.M.R Hutchinson and W.B. Mann and P.A. Mullen, NIM, 112 (1973) 187–196.

[27] I.J. Kim and C.S. Park and H.D. Choi, Appl. Rad. Isot, 58 (2003) 227–233.

[28] T. Vidmar, et al., Appl. Rad. Isot, 67 (2009) 160.

[29] K. Siegbahn, Alpha–, Beta– and Gamma–ray Spectroscopy, North Holland (1965).

[30] T. Lauritsen, et al., Phys.Rev. C, 75 (2007) 064309.

[31] G. Duchene, et al., Nucl. Instr. Meth. A, 432 (1999) 90–110.

[32] E. Farnea, Nucl. Instr. Meth. A, 621 (2011) 331 – 342.

[33] J. Ljungvall et al., to be published.

[34] P. Soderstrom, et al., Nucl. Instr. Meth. A, 638 (2011) 96 – 109.

[35] J. Dudouet, to be published.

[36] J. Gerl et al., to be published, (2016).

[37] T. Lauritsen and A. Korichi *et al.*, to be published.

[38] A. Korichi et al., in preparation.

[39] URL http://physics.nist.gov/PhysRefData/XrayMassCoef/chap2.html.